Nanomechanics of carbon nanofibers: Structural and elastic properties

Chenyu Wei[a] and Deepak Srivastava
NASA Ames Research Center, MS 229-1, Moffett Field, California 94035

(Received 3 May 2004; accepted 13 July 2004)

A general analytic expression for the Young's modulus of a range of carbon nanofibers (CNFs) with single or multishell nanocone or cone stacked structures has been developed from continuum elastic theory. The Young's modulus of a single-shell nanocone is found to be $\cos^4\theta$ of that of an equivalent single-wall carbon nanotube (CNT). The CNFs of short lengths and small tilting angles have very large Young's modulus comparable to that of single or multiwall CNTs, whereas the inverse is true for the CNFs with long lengths and large tilting angles. The dependence of the stiffness of CNFs on various structural parameters has been predicted by the model, validated through full-scale molecular dynamics simulations, and categorized for scanning probe tip or reinforcing fiber type applications. © *2004 American Institute of Physics*.
[DOI: 10.1063/1.1792797]

Numerous nanostructures composed of graphitic layers, including fullerenes, carbon nanotubes (CNTs), and carbon nanofibers (CNFs), have been subject of extensive experimental and theoretical studies for their unique properties. CNFs are generally the main products in many experiments, such as chemical vapor/catalytic deposition processes, and floating reactant production systems under certain conditions.[1–7] The graphitic shells in CNFs have conical structures with the shells at an angle to the axis of fibers. Experiments have also shown rather complicated structures of CNFs, where both cone stacked and bamboo structures are observed.[3,8,4,9] Despite the complex characteristic from applications perspective CNFs have advantages of better controllability of their location and size as compared with single-wall (SWCNTs) or multiwall CNT (MWCNTs).[10,11] Recently CNFs have been studied for their applications in reinforcement of composite materials, scanning probe nanotips and hydrogen storage, etc.[12,13] The mechanical properties of CNFs thus are important for their effectiveness in such applications, and are investigated in this work through continuum elastic theory and molecular dynamics (MD) simulations.

A schematic figure of the growth of CNFs is shown in Fig. 1, where the metal catalyst is on the bottom. There are four independent structural parameters defining a CNF, which are the length L, outer radius R_1, inner radius R_2, and tilting angle θ as shown in the figure. The three rectangles in Fig. 1 represent three different structural conditions. The corresponding three structural categories for CNFs can be defined depending on the relative magnitudes of L, R_1, R_2, and θ. For long fibers satisfying $L>(R_1-R_2)/\tan\theta$, CNFs have cone stacked structures with lots of open edges along the fiber axis [see Fig. 3(b) as an example]. For short fibers satisfying $L\leqslant(R_1-R_2)/\tan\theta$, CNFs have single or multishell nanocone structures [see Figs. 3(a) and 3(c) as examples], which can be further categorized as: single-shell nanocones with $(R_1-R_2)\leqslant h_0/\cos\theta$, and multishell nanocones with $(R_1-R_2)>h_0/\cos\theta$, with h_0 as the equilibrium distance between planes in graphite. SWCNTs or MWCNTs are the limiting cases of the single or multishell nanocones with $\theta\rightarrow 0$.

For a single-shell nanocone (Fig. 2) under a stress along the cone axis, coordinates are defined such that X and Y are along the radial directions and Z is along the cone axis, with the corresponding strains as ϵ_x, ϵ_y, and ϵ_z. As C–C bonds on the tilted graphene plane take the actual load, the axial strain, and the length of the cone and its change along the graphene plane are introduced as $\epsilon_{z,\|}$, $L_\|$ and $\delta L_\|$, respectively. Geometric considerations show that $L_\|+\delta L_\|=\sqrt{(L\tan\theta)^2(1-\gamma\epsilon_z)^2+(L+\delta L)^2}$, where $\gamma=-\epsilon_{x,y}/\epsilon_z$ is the Poisson ratio, and δL is change of length L along the Z axis. The relation between ϵ and $\epsilon_\|$ thus can be expressed as

$$\epsilon_{z,\|}=\frac{\delta L_\|}{L_\|}=(\cos^2\theta-\gamma\sin^2\theta)\epsilon_z+O(\epsilon_z^2). \tag{1}$$

Omitting the higher order terms in ϵ, a corresponding relation for the Poisson ratio along the graphene plane can be expressed as $\gamma_\|=-\epsilon_r/\epsilon_{z,\|}=-\epsilon_{x,y}/\epsilon_{z,\|}=\gamma/(\cos^2\theta-\gamma\sin^2\theta)$, where ϵ_r is the strain in the radial direction. By neglecting

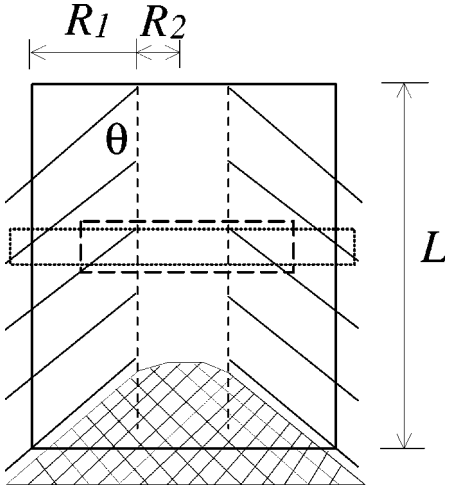

FIG. 1. Schematic illustration of a nanofiber (thick solid lines) composed of shells of nanocone with a tilting angle θ. The three rectangles represent three structural categories: cone-stacked (solid lines), single-shell (dashed lines) or multishell structures (dotted lines), respectively.

[a]Electronic mail: cwei@nas.nasa.gov

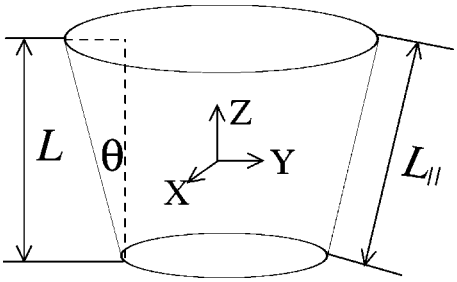

FIG. 2. Schematic illustration of a single-shell nanocone. See the text for definitions of the coordinates and parameters.

the higher order terms in γ, the Poisson ratio is further written as[14]

$$\gamma = \gamma_{\|} \cos^2 \theta. \tag{2}$$

As the strain energy $E=\frac{1}{2}k\epsilon^2$ can be equivalently expressed as a function of ϵ_z or $\epsilon_{z,\|}$, the corresponding relation for the force constant k and its counterpart $k_{\|}$ in the graphene plane can be written as $k=k_{\|}\cos^4\theta(1-\gamma_{\|}\sin^2\theta)^2$, considering Eq. (1). The Young's modulus of a single-shell nanocone is thus expressed as,

$$Y_{\text{cone}} = Y_{\text{SWNT}} \cos^4 \theta(1 - \gamma_{\|} \sin^2 \theta)^2, \tag{3}$$

where Y_{SWNT} is the Young's modulus of SWCNTs and the wall thickness of the cone and the SWCNT is assumed the same as h_0.

In a general case, a CNF is composed of N shells of nanocones, with either cone-stacked or multishell structures. When an external strain is applied on the CNF, the load can be carried partially by each shell and partially by the interfacial van der Waals (VDW) interactions. The total strain energy of a CNF can therefore be expressed as

$$E = AL\frac{1}{2}Y\epsilon^2 = \sum_{i=1}^{N} E^i_{\text{shell}} + \sum_{i=1}^{N-1} E^{i,i+1}_{\text{VDW}}, \tag{4}$$

where Y and A are the Young's modulus and cross-section area of the nanofiber. The strain energy on each shell i is $E^i_{\text{shell}}=\frac{1}{2}Y_sA_sL_s(\epsilon^i_s)^2$, where Y_s, A_s, L_s, and ϵ^i_s are Young's modulus, cross-section area, length, and induced strain on each individual shell, respectively. The strain energy contributed by the VDW interaction between shells i and $i+1$ is $E^{i,i+1}_{\text{VDW}}=\frac{1}{2}k_gA^{i,i+1}_g(\delta h)^2$, where k_g, $A^{i,i+1}_g$, and δh are force constant, surface area for VDW interactions, and displacement from the equilibrium distance between the graphene planes along the normal direction, respectively. All the structural parameters in the above noted expressions are related to the four basic structural parameters L, R_1, R_2, θ as $A_s=2\pi R_sh_0=\pi(R_1+R_2)h_0$; $L_s=(R_1-R_2)/\sin\theta$; and $\delta h=\delta L\sin\theta=h_0\epsilon$. The surface area for VDW interactions is defined as $A^{i,i+1}_g=s_{i,i+1}\times(R_1+R_2)(R_1-R_2)/\sin\theta$, where a pre-factor $s_{i,i+1}\in[0,1]$ is introduced, with $s_{i,i+1}\to 1$ for $\theta\to\pi/2$ and $s_{i,i+1}\to 0$ for $\theta\to 0$. Using the above noted expressions in Eq. (4), the Young's modulus of a N-shell CNF can be expressed as

$$Y = Y_s\frac{\sum_i(\epsilon^i_s/\epsilon)^2}{N} + k_gh_0\sum_{i=1}^{N-1} s_{i,i+1}\frac{\Delta L}{L}, \tag{5}$$

where ΔL is the equilibrium intershell distance along the nanofiber direction. The first term in Eq. (5) provides a strong mechanical response to the external load due to the strong sp^2 bonding in graphene planes, whereas the second term due to the VDW interactions is rather weak. This is validated through MD simulations, and is discussed in the following. The details of MD simulations were described elsewhere.[15]

Shown in Fig. 3(a) is a large angle nanocone with $\theta=30°$, $R_1\sim 15$ Å, $R_2\sim 3$ Å, and $L\sim 20$ Å. Axial strains of up to 5% were applied to the nanocone. Neglecting the radii change due to the Poisson ratio effect, the force constant for the nanocone is found to be $\partial^2E/\partial\epsilon^2=25.70$ eV/atom. Similar MD simulations have shown that $\partial^2E/\partial\epsilon^2=45.70$ eV/atom on straight SWCNTs, and the value does not depend strongly on the radius and chiralty for $r>3.5$ Å. Using the MD simulated force constants in the relation $Y_{\text{cone}}\simeq Y_{\text{SWNT}}\cos^4\theta$ [with $\gamma=0$ in Eq. (3)], a value of $\theta=30.01°$ is obtained, which is in excellent agreement with $\theta=30°$ from the geometry shown in Fig. 3(a). Similarly, the MD simulated $\gamma\approx 0.25$ for the nanocone is in excellent agreement with $\gamma\approx 0.23$ as predicted by Eq. (2) for $\gamma_{\|}\approx 0.30$ simulated for large diameter SWCNTs. The MD simulations thus validate Eqs. (2) and (3) for the single-shell nanocone described earlier.

The full MD simulations were also conducted on a CNF with four shells of nanocones stacked together [Fig. 3(b)]. The intershell interaction is only through VDW interactions. The initial structure was relaxed at zero strain, and external strains of up to 5% were applied on the nanofiber. The Young's modulus is found to be 0.03 TPa, which is much smaller than the typical Young's modulus of SWCNTs ($\sim$1 TPa).[16] The load transferred to each shell is negligible [$\epsilon_i\sim 0$ in Eq. (5) for this structure], and the weak VDW interactions bear most of the load, resulting in a very weak Young's modulus.

Shown in Fig. 3(c) is a seven-shell CNF, with $R_1\sim 24$ Å, $R_2\sim 5$ Å, $L\sim 41$ Å, and $\theta\sim 10°$. MD simulations were performed for the stress–strain responses (with ϵ up to 5%), in which the external load was applied only onto the outermost three shells. The contributions from the inner shells are mainly through VDW interactions and remain very small. Net Young's modulus of the overall CNF in Fig. 3(c) is found to be 0.5 TPa. This is in agreement with Eq. (5) which can be approximated as $Y\sim Y_s(M/N)$, where M is

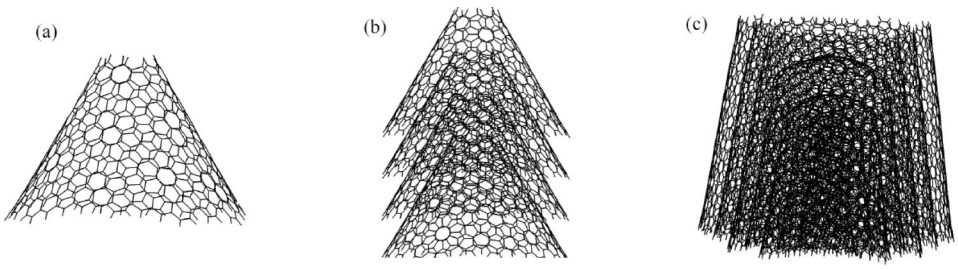

FIG. 3. Three structural types of carbon nanofiber: (a) A single-shell nanocone with $\theta=30°$; (b) A four-nanocone-stacked CNF with each individual shell the same as in (a); and (c) A seven-shell CNF, with $\theta\sim 10°$.

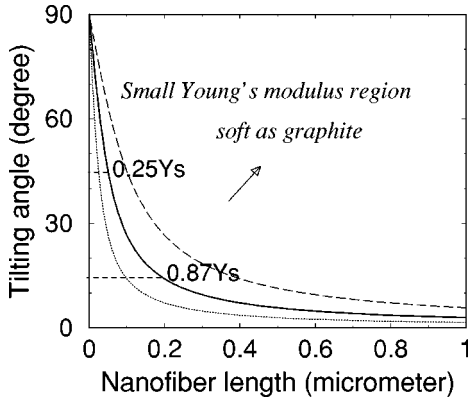

FIG. 4. The domains of nanocone stacked and single/multishell CNFs as functions of tilting angle θ and length, divided by curves of $L\times\tan\theta=(R_1-R_2)$. Three cases of $(R_1-R_2)=25$ nm (dotted line), 50 nm (solid line), and 100 nm (dashed line) are shown. The single/multishell CNFs of $\theta\sim15°$ and 45° with modulus ~0.87, 0.25 of that of straight CNT are marked.

number of shells bearing load, N is the number of total shells in the structure, and $Y_s\sim Y_{\mathrm{SWNT}}\sim1$ TPa as θ is very small in this case.

The correlations between the mechanical properties and the structures of CNFs are further illustrated in Fig. 4. The X axis shows the variation in the length of CNFs up to 1 μm and Y axis is for the titling angle of shells ranging from 0 to $\pi/2$. The curves of $L\times\tan\theta=(R_1-R_2)$ are shown for three cases of $(R_1-R_2)=25$, 50, and 100 nm, which separates the overall response into two structural domains. The bottom-left region satisfying $L\times\tan\theta\leqslant(R_1-R_2)$ represents single or multishell nanocone structured CNFs with large Young's modulus, whereas the top-right region satisfying $L\times\tan\theta>(R_1-R_2)$ represents cone-stack structured CNFs with very small Young's modulus. As seen from Fig. 4, for fixed radius, a short length of CNFs and a small titling angle leads to large Young's modulus values. The Young's modulus of single or multishell nanocone structured CNFs itself depends on the titling angle as shown in Eq. (3), which is marked in Fig. 4 for $\theta\sim15°$ and 45° (omitting the effect of γ). The bottom-left region could be suggested for the applications of CNFs with mechanical properties comparable to CNTs. For example for a 1-μm-long CNF of mean diameter 50 nm, a tilting angle smaller than 7° is needed to have a Young's modulus comparable to SWCNTs.

In summary, we have studied the mechanical properties of CNFs through continuum elastic theory and MD simulations, and found that the structures of CNFs can be defined into three categories. The Young's modulus of a single-shell nanocone is found to have a ratio of $\cos^4\theta$ as compared with that of a straight CNT, with a small correction from the Poisson ratio effect. A general expression for the Young's modulus of CNFs extending from a single-shell nanocone to multishell nanofiber is derived from continuum elastic theory and validated by detailed MD simulations. CNFs with short length and small titling angle are predicted to have relatively large Young's modulus, whereas CNFs with long length and large titling angle are expected to be soft graphitic type materials.

The authors would like to thank L. Chernozetonskii and M. Menon for providing the atomic structure shown in Fig. 3(c). NASA support to UARC through Contract No. NAS2-03144 is acknowledged.

[1]N. M. Rodriguez, J. Mater. Res. **8**, 3233 (1993).
[2]Z. F. Ren, Z. P. Huang, J. W. Xu, J. H. Wang, P. Bush, M. P. Siegal, and P. N. Provencio, Science **282**, 1105 (1998).
[3]V. I. Merkulov, D. H. Lowndes, Y. Y. Wei, G. Eres, and E. Voelkl, Appl. Phys. Lett. **76**, 3555 (2000).
[4]M. Endo, Y. A. Kim, T. Hayashi, Y. Fukai, K. Oshida, M. Terrones, T. Yanagisawa, S. Higaki, and M. S. Dresselhaus, Appl. Phys. Lett. **80**, 1267 (2002).
[5]K. Mathews, B. Cruden, B. Chen, M. Meyyappan, and L. Delzeit, J. Nanosci. Nanotechnol. **2**, 475 (2002).
[6]A. V. Melechko, T. E. McKnight, D. K. Hensley, M. A. Guillorn, A. Y. Borisevich, V. I. Merkulov, D. H. Lowndes, and M. L. Simpon, Nanotechnology **14**, 1029 (2003).
[7]S. Helveg, C. Lopez-Cartes, J. Schested, P. L. Hansen, B. S. Clausen, J. R. Rostrup-Nielsen, F. Abild-Pedersen, and J. K. Norskov, Nature (London) **427**, 426 (2004).
[8]T. Katayama, H. Araki, and K. Yoshino, Appl. Phys. Lett. **91**, 6675 (2002).
[9]M. Endo, Y. A. Kim, M. Ezaka, K. Osada, T. Yanagisawa, T. Hayashi, M. Terrones, and M. S. Dresselhaus, Nano Lett. **3**, 723 (2003).
[10]V. I. Merkulov, M. A. Guillorn, D. H. Lowndes, M. L. Simpson, and E. Voelkl, Appl. Phys. Lett. **79**, 1178 (2001).
[11]V. I. Merkulov, D. H. Hensley, A. V. Melechko, M. A. Guillorn, D. H. Lowndes, and M. L. Simpson, J. Phys. Chem. B **106**, 10570 (2002).
[12]K. Lozano and E. V. Barrera, J. Appl. Polym. Sci. **79**, 125 (2001), and references therein.
[13]A. Chambers, C. Park, R. Terry, K. Baker, and N. Rodriguez, J. Phys. Chem. B **102**, 4253 (1998).
[14]The Poisson ratio of CNT($\sim\gamma_{\|}$) is expected to have a slight dependence on the radius and chiralty for large diameter tubes, which effect is omitted in Eq. (2).
[15]C. Wei, K. Cho, and D. Srivastava, Phys. Rev. B **67**, 115407 (2003); C. Wei, K. Cho, and D. Srivastava, Appl. Phys. Lett. **82**, 2512 (2003).
[16]For reviews see D. Srivastava, C. Wei, and K. Cho, Appl. Mech. Rev. **56**, 215 (2003).